J Mater Sci (2009) 44:4776–4780
DOI 10.1007/s10853-009-3718-y

Study on graphite fiber and Ti particle reinforced Al composite

G. H. Wu · J. Su · H. S. Gou · Z. Y. Xiu ·
L. T. Jiang

Received: 1 June 2009 / Accepted: 1 July 2009 / Published online: 28 July 2009
© Springer Science+Business Media, LLC 2009

Abstract Graphite fiber and Ti particle-reinforced aluminum matrix composite were produced by squeeze casting technology. A small amount of needle aluminum carbide at graphite fiber and Al interface was observed, and $TiAl_3$ intermetallic compound at Ti particle and Al interface was detected. Tensile strength and bending strength of the composite have been measured. The fracture surface of the composite after tensile and bending tests was observed; graphite fiber-reinforced Al was brittle fracture, whereas Ti particle-reinforced Al was ductile fracture. The corresponding fracture mechanism was discussed.

Introduction

In the past years, there has been significant interest in particle and fiber-reinforced composite materials, which has largely been stimulated by exploiting metal matrix composites (MMCs) systems [1–4]. Continuous graphite-fiber reinforced aluminum composites (Gr_f/Al) are one type of MMCs that have attracted the interest of composite manufacturers and researchers, due to their high specific strength, high specific stiffness, low coefficient of thermal expansion, and high thermal conductivity [5–7]. These properties make Gr_f/Al composite candidates for a wide range of applications in astronautic and aeronautic industries.

The main factors affecting properties of Gr_f/Al composite are matrix alloy and interface bonding [8]. Some common aluminum alloys are chosen as the matrix for the composite [9–11], and the alloy elements will affect interface reactant and mechanical properties of the composite. In this study, pure aluminum is chosen as the matrix. During the fabricating of the composite, the main problems are non-wetting conditions between graphite fiber and Al matrix [12], and the undesirable formation of aluminum carbides (Al_4C_3) at the interface. In order to avoid the non-wetting and reduce the thermal expansion mismatch between graphite fiber and Al matrix, Ti particles are introduced into the composite.

Ti is especially interesting because of its low density, high elastic modulus, high specific strength, and good fatigue properties [13]. Additional beneficial effect of titanium addition results from its plastic deformation, in such a way that part of the load might be transferred plastically to the Ti reinforcement [14]. Ti has been extensively used in aerospace and sports industries. However, Ti has not been used as a particulate-reinforcing material in the Gr_f/Al composite, although there is a study of using Ti particle as reinforcement in Al [15].

This study investigated the tensile strength and bending strength of graphite fiber and Ti particle-reinforced Al (Gr_f + Tip/Al) composite, which was processed by squeeze casting. The microstructure and the failure mechanism of the composite were discussed.

G. H. Wu (✉) · J. Su · H. S. Gou · L. T. Jiang
School of Materials Science and Engineering, Harbin Institute of Technology, P.O. Box 3023, Science Park, No. 2 Yikuang Street, Harbin, Heilongjiang 150080, People's Republic of China
e-mail: wugh@hit.edu.cn

J. Su
e-mail: susoc@163.com

Z. Y. Xiu
Research Academy of Science and Industry Technology, Harbin Institute of Technology, P.O. Box 3023, Science Park, No. 2 Yikuang Street, Harbin, Heilongjiang 150080, People's Republic of China

Materials and experimental methods

The basic properties of graphite fiber are shown in Table 1. They have been selected as the fiber reinforcement for their high modulus and high strength. The volume content of the graphite fiber in the composite is about 50 vol.%. Ti particles were selected as the particle reinforcement. The morphology of graphite fibers and Ti particles is shown in Fig. 1a, b, respectively. The diameter of graphite fiber was about 5–6 μm, and some grooves paralleling to fiber-axis in their surface were observed. The average diameter of Ti particle was about 11 μm (≥98 wt%), and irregular shape was detected. High-purity aluminum (99.99 wt%) was used as the matrix. The Gr_f + Tip/Al composite was processed by squeeze casting.

Morphology of the composite and fractured surface of tensile and bending specimens were observed using an S-4700 scanning electron microscopy (SEM). X-ray diffraction (XRD) was performed using Philips X'pert XRD device for phase analysis, and the patterns were compared with standard spectra from powder diffraction files. The interfacial microstructure of the composite was observed by a Philips T20 transmission electron microscopy (TEM) with an accelerating voltage of 200 kV. Energy dispersive X-ray (EDX) was used to identify and calculate the approximate elemental composition of products. The specimens paralleling to the fiber direction were chosen for tensile tests (tensile specimen dimensions are shown in Fig. 2) and the three-point bending tests (specimen dimensions of $2 \times 10 \times 60$ mm^3) at room temperature using INSTRON 5569 universal test machine (100 kN static load capacity), and the loading rate was 0.5 mm/min. Mechanical properties' test samples were detected by radiography.

Table 1 Basic properties of graphite fiber

Tensile strength (GPa)	Young's modulus (GPa)	Fracture elongation (%)	Density (g/cm^3)
4.41	377	1.2	1.77

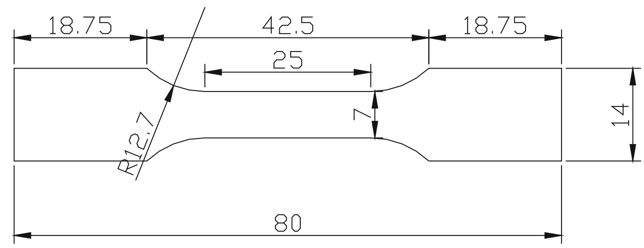

Fig. 2 Dimensions of tensile test sample

Results and discussion

Microstructure and phase analysis

Figure 3a shows typical micrograph of Gr_f + Tip/Al composite. The composite was free from common cast defects, such as porosities and shrinking cavities. It was beneficial to the improvement in mechanical strength. No interphase product was observed around Ti particles and graphite fibers by SEM.

XRD pattern of the composite was shown in Fig. 3b. C, Al, and Ti diffraction peaks were observed without interface reactant.

Figure 4 shows TEM micrographs of Gr_f + Tip/Al composite. Needle-shaped reaction product of aluminum carbide (Al_4C_3) was found at the interface of graphite fiber and Al, as shown in Fig. 4a. Al_4C_3 is often observed in C/Al composites. At 670 °C, the free energy of formation of Al_4C_3 is −176 kJ/mol [16]. Compared with the C and Al interface, Ti–Al intermetallic compound phase was observed at the interface of Ti particle and Al, as shown in Fig. 4b. EDX result shows that the atom ratio of Ti to Al is about 1:3, which indicates that the product was $TiAl_3$. The result is consistent with the study of Hsu et al. [17].

Mechanical properties

Mechanical properties' samples were detected by radiography, and the results are shown in Figs. 5 and 6. All

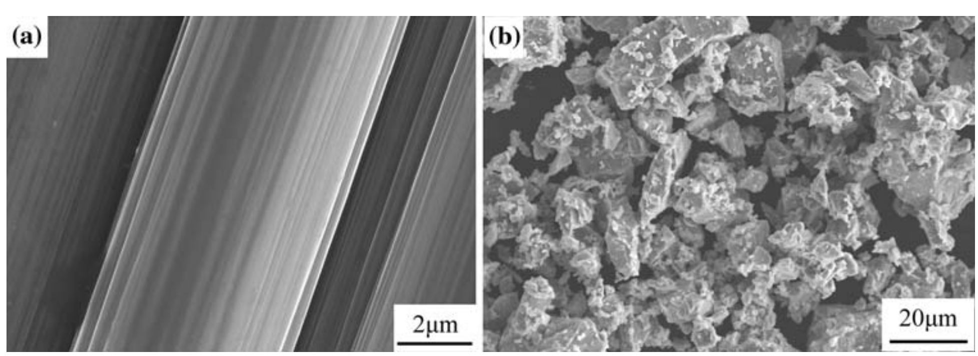

Fig. 1 The morphology of **a** graphite fiber, **b** Ti particle

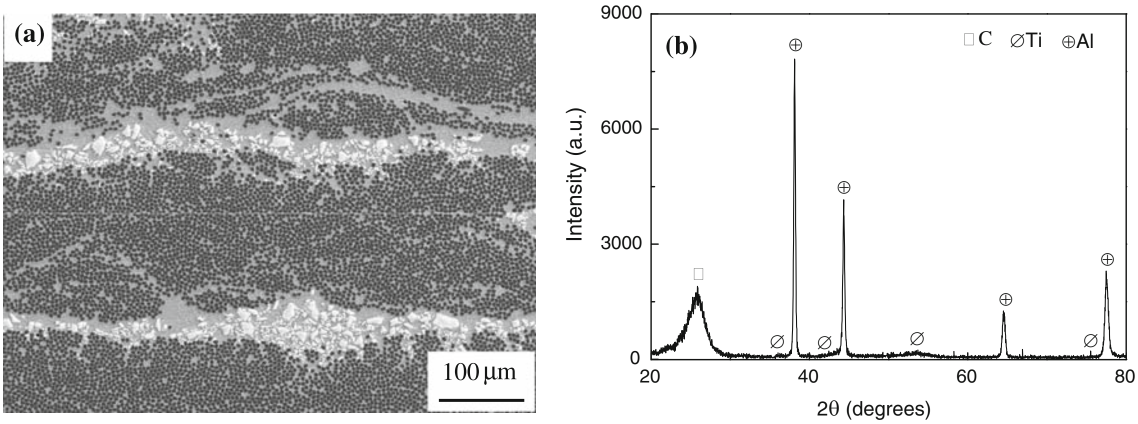

Fig. 3 Typical optical micrograph and XRD pattern of Gr_f + Tip/Al composites. **a** Optical micrograph, **b** XRD pattern

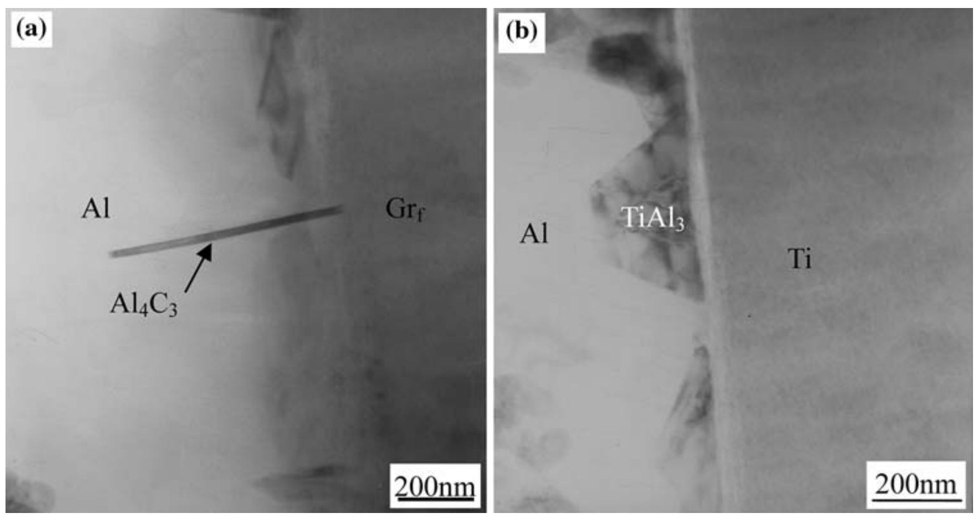

Fig. 4 TEM micrographs of Gr_f + Tip/Al composites. Interfacial reaction products of **a** Al_4C_3, **b** $TiAl_3$

samples are dense without porosity and shrinkage cavity. Graphite fibers distribute uniformly and straightly.

Mechanical properties of Gr_f + Tip/Al composites in this study and relative experiment results [15, 18] are presented in Table 2. The results indicate that mechanical properties and elastic modulus of the composite were improved by reinforcement, which can be attributed to the contribution of: (a) smaller size of the Ti particles and (b) high modulus and strength of graphite fibers.

Figures 7 and 8 show the tensile and bending fracture surfaces of Gr_f + Tip/Al composite at room temperature, respectively. Figures 7b and 8b show that the fracture surface of graphite fiber and Al was flat and no fiber pullout. The flatness of the fracture surfaces reflects the rapid propagation of failure in the composites. It is commonly considered that good mechanical properties of composite is attributed to an intermediate interfacial bonding, either strong or weak interfacial bonding may lead to composite strength decreasing [19]. Interfacial bonding of graphite fiber and Al in current composite is

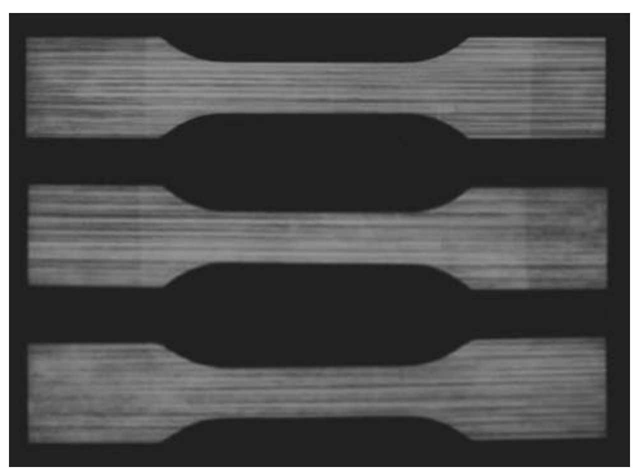

Fig. 5 Radiography result of tensile test samples

still relatively stronger than optimized one, which result in lower tensile strength. During loading, these brittle Al_4C_3 may break before the fiber due to strong interface

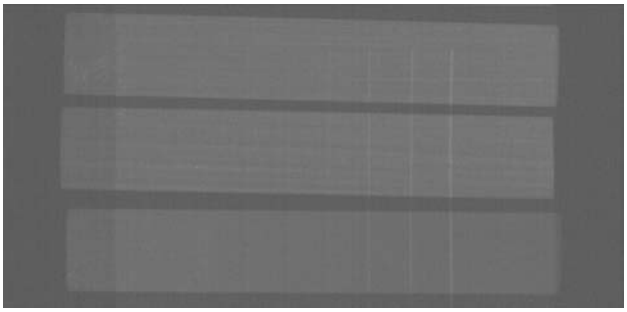

Fig. 6 Radiography result of bending test samples

Table 2 Mechanical properties of Gr_f + Tip/Al composites and other reported experiment results

Material	Bending strength (MPa)	Tensile strength (MPa)	Elastic modulus (GPa)	Document
Pure Al	–	118	68	15
Gr_f/Al	405	373	259	18
7.5 wt%Tip/Al	–	146	85	15
Gr_f + Tip/Al	562	239	190	This study

bonding, then become crack initiated, and the corresponding crack may propagate in the fiber and the surrounding aluminum matrix, finally result in low stress fracture of composites.

Figures 7c and 8c show that the fractured surfaces of Ti particle and Al exhibited a ductile fracture mode. Ti particle fracture and debonding were observed at the interface of Ti particle and Al. Ti particle breakage indicates the effective transfer of the load from the matrix to the reinforcement. The presence of tearing edges on the fracture surface indicates that the intermediate interfacial bonding obtained between the Ti particle reinforcements and the Al matrix in the composite.

Conclusions

According to the above results, the following conclusion could be drawn:

(1) Gr_f + Tip/Al composites were well infiltrated with no apparent porosity and significant casting defect.

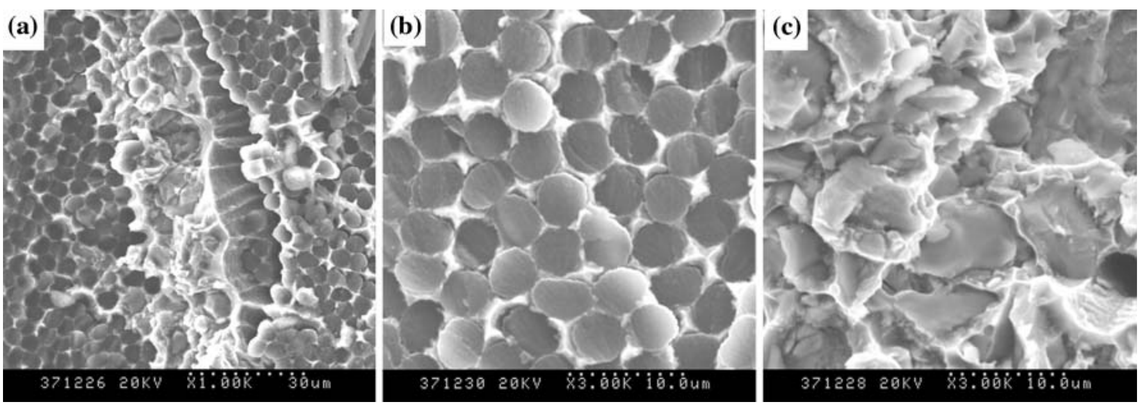

Fig. 7 The fracture surface of tensile test samples. **a** Overall view of the tensile fracture surface, **b** high magnification of graphite fiber and Al, **c** high magnification of Ti particle and Al

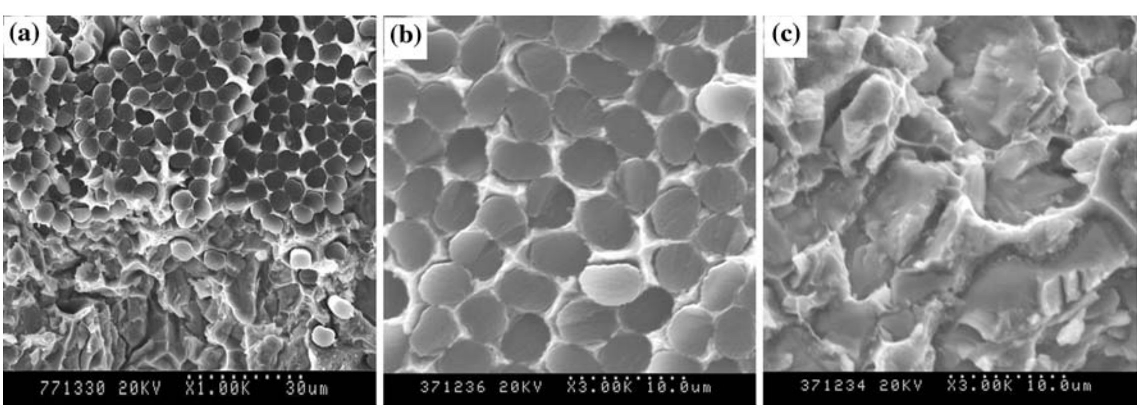

Fig. 8 The fracture surface of bending test samples. **a** Overall view of the bending fracture surface, **b** high magnification of graphite fiber and Al, **c** high magnification of Ti particle and Al

(2) Gr_f + Tip/Al composites showed needle-shaped Al_4C_3 at the interface of graphite fiber and Al, and $TiAl_3$ phase at the interface of Ti particle and Al.

(3) Tensile strength and bending strength of Gr_f + Tip/Al composites increased compared to the Al matrix, which could attribute to high modulus and high strength graphite fiber, and intermediate interfacial bonding between Ti particle and Al.

References

1. Zhou YX, Wen HA, Xia YM (2002) Compos Sci Technol 62:1935
2. Matsunaga T, Ogata K, Hatayama T (2007) Composites Part A 38:771
3. Lu Y, Hirohashi M, Pan F (2004) J Mater Sci 39:969. doi:10.1023/B:JMSC.0000012929.27601.33
4. Wang YQ, Yang JY, Wang ZM, Zhou BL (1995) Chin J Mater Res 9(3):279
5. Seong HG, Lopez HF, Robertson DP (2008) Mater Sci Eng A 487:201
6. Zhou YX, Wang Y, Xia YM, Mallick PK (2003) Mater Sci Eng A 362:112
7. Yoshida M, Matsunaga T, Ogata K, Hatayama T, Shinozaki K (2007) Mater Sci Forum 539–543:877
8. Zhang GG, Luo SJ, Tian WT (2002) Chin J Nonferrous Met 12(3):525
9. Daoud A (2005) Mater Sci Eng A 391:114
10. Matsunaga T, Ogata K, Hatayama T, Shinozaki K, Yoshida M (2006) In: Solidification processing of metal matrix composites symposium: processing and microstructure of MMCs – I, San Antonio, Texas, pp 123–132
11. Chu SJ, Wu RJ (1998) Mater Eng 6:17
12. Landry K, Kalogeropoulou S, Eustathopoulos N (1998) Mater Sci Eng A 254:99
13. Hassan SF, Gupta M (2002) J Alloys Compd 345(1–2):246
14. Perez P, Garces G, Adeva P (2004) Compos Sci Technol 64(1):145
15. Sanjay KT, Manoj G (2007) Composites Part A 38:1010
16. Etter T, Schulz P, Weber M, Metz J (2007) Mater Sci Eng A 448(1–2):1
17. Hsu CJ, Chang CY, Kao PW, Ho NJ, Chang CP (2006) Acta Mater 54:5241
18. Wang X, Chen GQ, Li B (2009) J Mater Sci. doi:10.1007/s10853-009-3639-9
19. Vidal-Se′tif MH, Lancin M, Marhic C (1999) Mater Sci Eng A 272:321